Int. J. Heat Mass Transfer. Vol. 7, pp. 549–568. Pergamon Press 1964. Printed in Great Britain

CONVECTIVE HEAT TRANSFER IN A CONVERGENT–DIVERGENT NOZZLE†

L. H. BACK,‡ P. F. MASSIER§ and H. L. GIER||
Jet Propulsion Laboratory, 4800 Oak Grove Drive, Pasadena, Calif.

(*Received* 2 *August* 1963 *and in revised form* 30 *October* 1963)

Abstract—The results of an experimental investigation of convective heat transfer from turbulent boundary layers accelerated under the influence of large pressure gradients in a cooled convergent–divergent nozzle are presented. The investigation covered a range of stagnation pressures from 30 to 250 psia, stagnation temperatures from 1030° to 2000°R, and nozzle-inlet boundary-layer thicknesses between 5 and 25 per cent of the inlet radius. The most significant unexpected trend in the results is the reduction in the heat-transfer coefficient, below that typical of a turbulent boundary layer, at stagnation pressures less than about 75 psia. As expected, the results include a maximum in the heat-transfer coefficient upstream of the throat where the mass flow rate per unit area is largest, and a substantial decrease of the heat-transfer coefficient downstream of the point of flow separation which occurred in the divergent section of the nozzle at the low stagnation pressures. A reduction of about 10 per cent in the heat-transfer coefficient resulted from an increase in the inlet boundary-layer thickness between the minimum and maximum thicknesses investigated.

Heat-transfer predictions with which the data were compared either incorporate a prediction of the boundary-layer characteristics or are related to pipe flow. At the higher stagnation pressures, predicted values from a modification of Bartz's turbulent-boundary-layer analysis are in fair agreement with the data. As a possible explanation of the low heat transfer at the lower stagnation pressures, a parameter is found which is a measure of the importance of flow acceleration in reducing the turbulent transport below that typical of a fully turbulent boundary layer.

NOMENCLATURE

- a, speed of sound;
- A, local nozzle cross-sectional area;
- A^*, nozzle throat area;
- c^*, characteristic velocity $p_0 A^* g_c/\dot{m}$;
- c_f, local wall friction coefficient, $c_f/2 = \tau_w/\rho_e u_e^2$;
- c_f^*, coefficient analogous to skin-friction coefficient, with momentum thickness dependence replaced by energy thickness;
- c_p, specific heat at constant pressure;
- D, nozzle diameter;
- D^*, nozzle throat diameter;
- g_c, gravitational constant;
- h, convective heat-transfer coefficient;
- l, cooled-approach length;
- L, axial length of nozzle = 5·925 in;
- $\dot{m}$, mass flow rate;
- M, Mach number;
- p, static pressure;
- p_t, stagnation pressure;
- Pr, Prandtl number;
- q_w, wall heat flux;
- $q^2/2$, turbulent kinetic energy;
- r, nozzle radius;
- r^*, nozzle-throat radius;
- r_c, nozzle-throat radius of curvature;
- R, nozzle-inlet radius = 2·53 in;
- Re_D, Reynolds number based on nozzle diameter, $\rho_e u_e D/\mu_e$;
- St, Stanton number, $h/\rho_e u_e c_p$;
- T, temperature;
- u, velocity component in the x direction;
- v, velocity component normal to wall;
- x, distance along the wall in the flow direction;
- y, distance normal to wall;

† Portions of this paper were originated under studies conducted for the Department of Army Ordnance Corps under Contract No. DA-04-495-Ord-18. Such studies are now conducted for the National Aeronautics and Space Administration under Contract No. NAS 7–100.

‡ Senior Research Engineer.

§ Research Group Supervisor.

|| Research Engineer.

z, axial distance from nozzle inlet.

Greek symbols

γ, specific-heat ratio;
δ, velocity boundary-layer thickness;
δ_t, stagnation-temperature boundary-layer thickness;
δ^*, displacement thickness;
θ, momentum thickness;
μ, viscosity;
ν, kinematic viscosity;
ρ, density;
σ, dimensionless property correction factor (defined in [20]);
τ_w, wall shear stress;
ϕ, energy thickness;
χ, parameter.

Subscripts

aw, adiabatic wall condition;
e, condition at free-stream edge of boundary layer;
f, property evaluated at film temperature, $T_f = (T_w + T_e)/2$;
i, j, components in Cartesian coordinates;
0, upstream reservoir condition;
t, stagnation condition;
w, wall condition;
1, one-dimensional flow value.

Superscripts

$(\ )'$, fluctuating component;
$\overline{(\ )}$, time average.

INTRODUCTION

COMPREHENSIVE studies of convective heat transfer from gases flowing under the influence of comparatively large pressure gradients have been mostly analytical. Laminar-flow cases have been solved by boundary-layer theory approaches in which the restrictive assumptions are within the realm of describing actual processes. Turbulent flows, however, are too complex to formulate in such a way that descriptions of the momentum and energy transport processes can be made without the use of considerable empirical information or assumptions which are so drastic that they themselves are essentially the solutions. The present investigation was undertaken in order to provide experimental convective heat-transfer information on turbulent flows subjected to large pressure gradients with boundary layers that are thin in comparison to the cross section of the channels. It was anticipated that these results could be incorporated with turbulent boundary-layer theories to arrive at a meaningful method of predicting convective heat transfer in accelerating flows.

Experimental measurements of heat transfer from gases flowing under the influence of pressure gradients have been made to some extent by other investigators. Data obtained from rocket-engine firings indicate that the local heat fluxes in nozzles (particularly the convergent sections) are sensitive to injection schemes, combustion phenomena, and the proximity of a nozzle to the injector [1]. Furthermore, superimposed on the convective component is a radiation component which, together with the other effects, introduces complexities into the gross heat-transfer process. Hence, results of measurements such as these have not been particularly informative about the convective heat-transfer mechanism in accelerating turbulent boundary-layer flows.

Most experimental results of previous investigations of convective heat transfer in a nozzle without injection and combustion effects were obtained either with nozzles of small angles of convergence and divergence or at relatively low stagnation pressures and temperatures. Saunders and Calder's measurements [2] were made only in the conical divergence section, with the half-angle of divergence about $\frac{1}{2}°$. Ragsdale and Smith [3], using superheated steam, made measurements in a nozzle which had small convergent and divergent half-angles of about 1°. The stagnation temperature was about 1000°R, and the stagnation pressure ranged from 20 to 35 psia. Baron and Durgin's measurements [4] in two-dimensional nozzles were made at a stagnation temperature of 570°R and over a stagnation pressure range from 6 to 30 psia. In preliminary results [5] from the system shown in Fig. 1, semi-local values of heat transfer were determined by calorimetry for a few operating conditions. Only for Kolozsi's measurements [6] in a $7\frac{1}{2}°$ half-angle convergent and divergent conical nozzle at a stagnation temperature of about 1200°R were data reported at higher stagnation pressures of 225 and 370 psia.

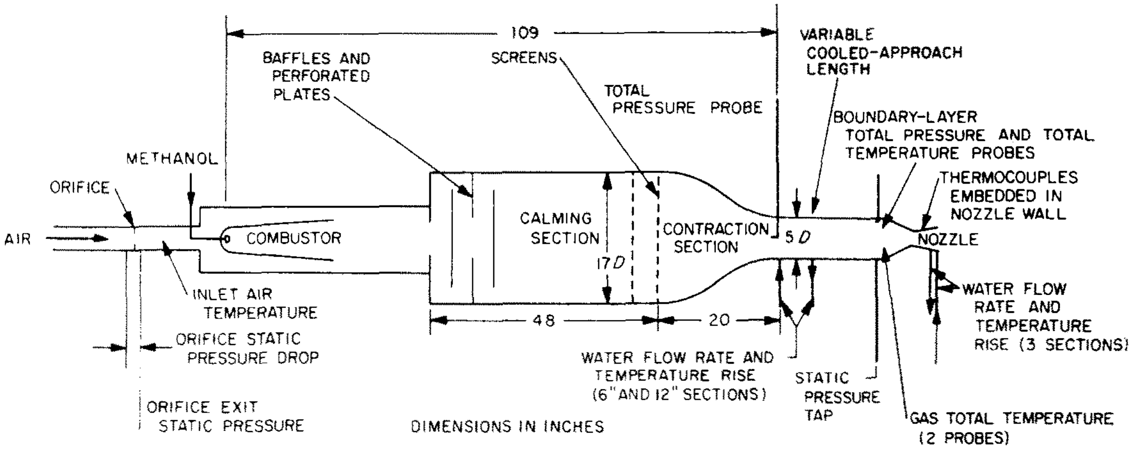

FIG. 1. Flow and instrumentation diagram.

In this investigation, compressed air was heated by the internal combustion of methanol and then mixed to obtain uniformity before it entered the nozzle. The mixing and distance of the combustion from the nozzle (Fig. 1) minimized maldistributions. The nozzle had a throat diameter of 1·803 in., a contraction-area ratio of 7·75 to 1, an expansion-area ratio of 2·68 to 1, a convergent half-angle of 30°, and a divergent half-angle of 15°. The exit Mach number was about 2·5. Local convective heat-transfer results were obtained by measuring steady-state temperatures with thermocouples embedded in the water-cooled nozzle wall. Radiation effects were negligible over the 1030° to 2000°R stagnation-temperature range. To determine the effect of boundary-layer thickness at the nozzle inlet on heat-transfer in the nozzle, the length of the constant-diameter cooled-approach section upstream of the nozzle inlet was changed in 6-in lengths from 0 to 18 in.

INSTRUMENTATION

The system flow and instrumentation diagram is shown in Fig. 1. The ratio of methanol-to-air weight flow rate was small enough, even for the highest stagnation temperature, so that the products of combustion could be treated approximately as air. Stagnation pressure was measured just upstream of the water-cooled approach section, and stagnation temperature was determined by averaging the readings of two shielded thermocouples located 0·25 in upstream of the nozzle inlet. These two thermocouples, located 1 in from the centerline, were spaced 180° apart circumferentially and generally read within 2 per cent of each other. To determine the static-pressure distribution along the nozzle, thirty-two static-pressure holes 0·040 in in diameter were spaced circumferentially and axially in the nozzle wall. These static pressures were measured with mercury manometers.

Boundary-layer traverses were made in the 5·07-in-diameter cooled-approach section at a location 1·25 in upstream of the nozzle inlet. The stagnation-pressure probe was located 90° circumferentially from the stagnation-temperature probe. Details of the probe tips are shown in Fig. 2. The tip design is similar to that of probes used by Livesey [7], with which he found a negligible velocity displacement effect of the probe in the wall vicinity.

To obtain the wall temperature and heat flux a thermocouple plug shown in Fig. 3 was located at each of twenty-one axial locations, except at $z/L = 0·864$ where there were two. These plugs were also spaced at numerous circumferential locations along the nozzle, as indicated in the table in Fig. 3, such that every third plug was located in a quadrant within 55° of successive ones. A technique for electrically determining the location of the thermocouple weld junctions was devised using a Kelvin bridge circuit. Three longitudinal water-coolant

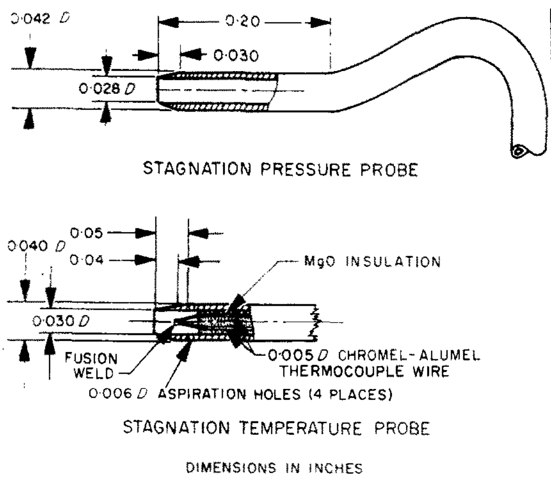

FIG. 2. Tip details of traversing boundary-layer probes.

passages were used to cool the outer surface of the nozzle and plugs.

HEAT-TRANSFER CALCULATION PROCEDURE

Although temperature gradients existed along the nozzle wall, these were generally small, and the three thermocouple readings in each plug indicated that only radial heat conduction normal to the wall need be considered. The gas-side wall temperatures determined from the different thermocouple combinations in each plug were generally within 1 per cent. However, in determining the wall heat flux, there were inconsistencies. If the center thermocouple and the one nearest the gas-side wall were used, the calculated wall heat flux was on the average about 10 per cent higher than when the thermocouples nearest the gas-side and water-side walls were used. With a combination of the center

Plug Position†

Plug No.	z/L	A/A^*	Circumferential angle from arbitrary zero (deg)
124	0·133	6·39	330
D25	0·204	5·05	30
D34	0·276	3·86	150
123	0·336	2·98	280
D26	0·385	2·37	80
D35	0·429	1·88	200
122	0·469	1·48	315
D28	0·512	1·23	45
H37‡	0·541	1·10	155
120§	0·573	1·02	300
D29	0·603	1·00	60
F42	0·634	1·02	180
119	0·664	1·08	285
D30	0·693	1·19	75
F43	0·717	1·28	200
118	0·750	1·41	320
D31	0·782	1·55	40
F45§	0·825	1·74	150
117	0·864	1·94	275
C16	0·864	1·94	320
D33	0·905	2·14	85
F46	0·938	2·41	205

† L = 5·925 in and A^* = 2·552 in² at z/L = 0·603.

‡ Data from this plug are questionable and have been omitted.

§ Water side wall thermocouple in this plug has been damaged.

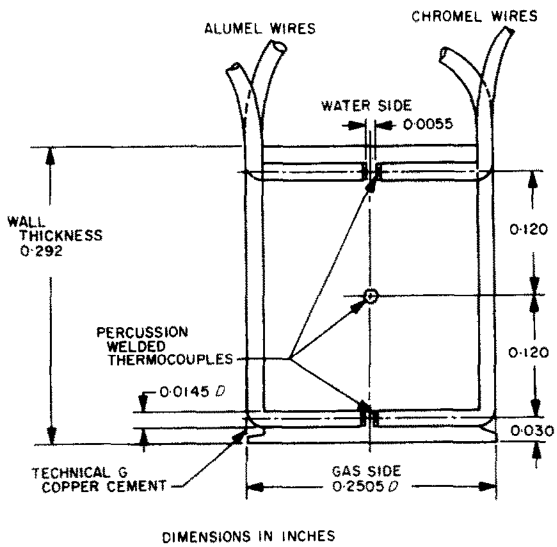

FIG. 3. Thermocouple plug diagram and positions.

thermocouple and the one nearest the gas-side wall, the total heat load was found to agree within 5 per cent of that computed from the coolant flow rate and the coolant temperature rise; consequently, these two thermocouples were used to calculate the wall heat flux.

The heat-transfer coefficient was computed by

$$h = \frac{q_w}{T_{aw} - T_w}.$$

The adiabatic wall temperature was calculated by taking the recovery factor equal to 0·89. This value is based on measurements with air accelerated over a flat plate by a convergent opposite wall [8] and by extrapolating wall temperatures to the zero heat flux condition for air flow through a nozzle [4]. In both of these investigations the recovery factor was found to be independent of pressure gradient. Actually for the large differences between the stagnation and wall temperatures in the present results the calculated heat-transfer coefficients are insensitive to the assumed recovery factor dependence.

STATIC PRESSURE AND MASS FLUX DISTRIBUTIONS

The measured static-to-stagnation pressure ratio along the nozzle is shown in Fig. 4 at a stagnation temperature of 1500°R for a range of stagnation pressures from 45 to 150 psia. Measurements at higher stagnation pressures were not possible because of manometer limitations. Except in the nozzle-exit region, where the rapid rise in static pressure at the lower stagnation pressures indicates flow separation, the pressure-ratio distribution is nearly invariant. For computational purposes, it is assumed to be invariant above 150 psia. Deviations of measured pressure distributions from that predicted from one-dimensional isentropic flow are indicated. Just downstream of the throat, these amount to 30 per cent. The deviations result from radial-velocity components caused by the taper and curvature of the nozzle.

In Fig. 5, the ratio of the local mass flux $\rho_e u_e$, calculated from the measured wall static pressures, to that predicted from one-dimensional flow $\rho_1 u_1$ is shown at $p_t = 75$ psia for different stagnation temperatures and cooled-approach lengths. For the tests shown, the maximum value of the mass flux $\rho_e u_e$ occurred at $z/L = 0{\cdot}58$. This location corresponds to the intersection of the sonic line with the nozzle wall and is upstream of the geometric throat, which is located at $z/L = 0{\cdot}603$. Just downstream of the throat, there is a sharp dip in the mass-flux ratio, the reduction below that predicted from one-dimensional flow amounting to about 15 per cent. There appears to be a slight trend toward mass-flux ratios increasing with stagnation temperature, especially near the nozzle exit. The effect of boundary-layer thickness at the nozzle inlet on the mass-flux ratio is negligible.

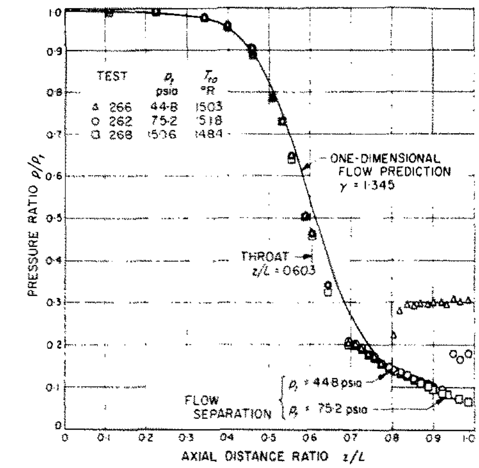

FIG. 4. Ratio of static to stagnation pressure along the nozzle.

Since the deviations from one-dimensional flow are significant in the throat region, it is of interest to determine to what extent the mass flux at the edge of the boundary layer is predictable. Oswatitsch and Rothstein [9] considered isentropic, two-dimensional flow in a converging–diverging nozzle. The wall boundary layer is neglected, as is the requirement that the fluid velocity at the wall be exactly parallel to it. The final result of their analysis can be cast in the form of a ratio of the mass flux at the nozzle wall to that for one-dimensional flow.

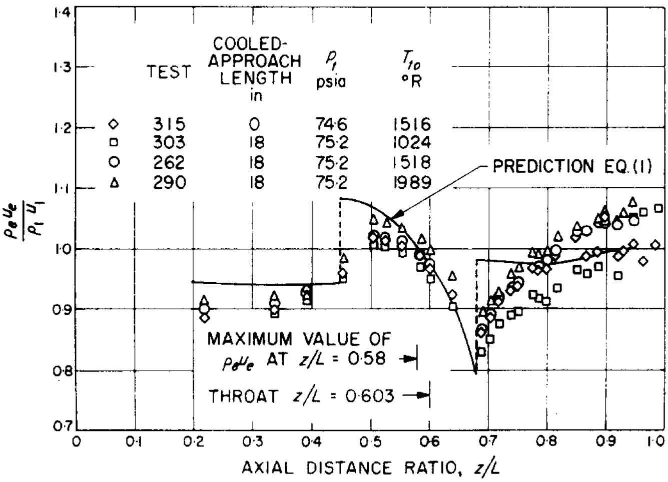

FIG. 5. Ratio of local to one-dimensional mass flux along the nozzle.

$$\frac{\rho_e u_e}{\rho_1 u_1} = \frac{\left[1 - \frac{\gamma - 1}{2}\left(M_1 \frac{a_1}{a_0}\right)^2 \left(\frac{u_e}{u_1}\right)^2\right]^{1/\gamma - 1}}{\frac{\rho_1}{\rho_0}} \left(\frac{u_e}{u_1}\right) \tag{1}$$

where

$$\frac{u_e}{u_1} = \sqrt{\left(\left\{1 + \frac{1}{2}\left[\frac{1}{2} r \frac{\mathrm{d}^2 r}{\mathrm{d}z^2} + \frac{1}{4}\left(\frac{\mathrm{d}u_1/\mathrm{d}z}{u_1}\right) r \frac{\mathrm{d}r}{\mathrm{d}z} - \left(\frac{\mathrm{d}r}{\mathrm{d}z}\right)^2\right]\right\}^2 + \left(\frac{\mathrm{d}r}{\mathrm{d}z}\right)^2\right)}.$$

The predicted mass-flux ratio is only a function of the nozzle geometry, with the subscript 1 denoting average quantities for one-dimensional flow. The prediction shown in Fig. 5 is in fair agreement with the data in the throat region. It also indicates the sonic line to be upstream of the throat. At the intersection of the conical sections of the nozzle with the throat curvature, there is a predicted discontinuity in the mass-flux ratio as indicated by the dashed lines. The prediction is not shown in the nozzle-entrance region since there, restrictions on the magnitude of the nozzle radius and its derivatives implied in the analysis are not satisfied. Even in the throat region, these are marginal.

BOUNDARY LAYERS AT THE NOZZLE INLET

To indicate the nature of the boundary layer at the nozzle inlet with the 18-in cooled-approach length, the velocity ratio u/u_e, mass-flux ratio $\rho u/\rho_e u_e$, and stagnation-temperature distribution $(T_t - T_w)/(T_{te} - T_w)$ are shown in Fig. 6 for a stagnation temperature of 1500°R and a range of stagnation pressures from 45 to 254 psia. The profiles indicate that the boundary layers are turbulent over the range of stagnation pressures. A $\frac{1}{7}$-power-law curve for negligible property variation across the boundary layer is shown for comparison. Values of the thicknesses δ^*, θ, and ϕ near the nozzle inlet were calculated by taking into account the mass, momentum, and energy defects for flow through a pipe of radius R. For example, the momentum thickness was calculated from

$$\theta\left(R - \frac{\theta}{2}\right) = \int_0^{\delta} \frac{\rho u}{\rho_e u_e}\left(1 - \frac{u}{u_e}\right)(R - y)\,\mathrm{d}y.$$

In general, these thicknesses are about 5 per cent lower than those obtained by assuming flow over a plane surface. The effect of increasing stagnation pressures is to decrease the displacement, momentum, and energy thicknesses.

At the other stagnation temperatures of 1030° and 2000°R, as well as with the shorter cooled-approach lengths of 6 and 12 in, the boundary-layer profiles, though not shown, were also turbulent. However, with no cooled-approach length, the boundary layer appears to be in the transition region, as indicated by the velocity

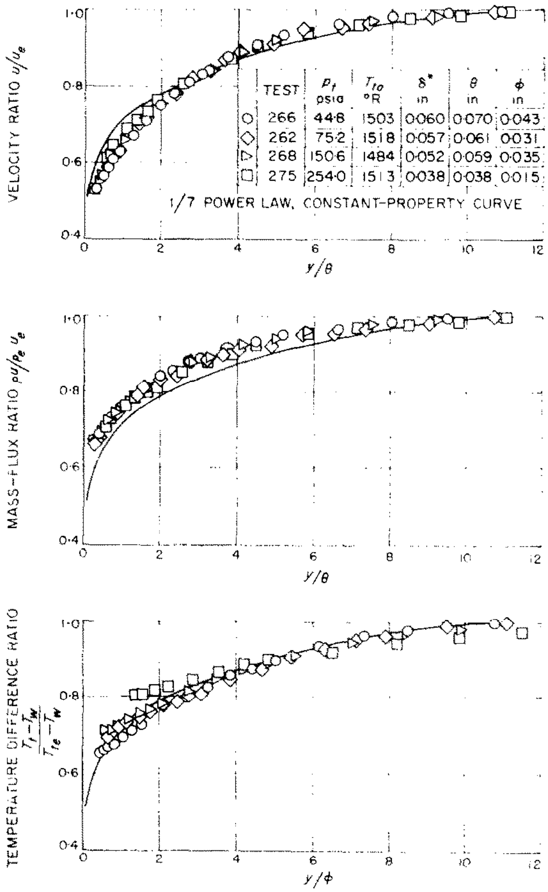

FIG. 6. Boundary-layer profiles 1·25 in upstream of the nozzle inlet with the 18-in cooled-approach length.

profiles shown in Fig. 7. These profiles lie between a turbulent and laminar one, as shown by the $_7$-power law and Blasius laminar-flow profiles.

HEAT-TRANSFER RESULTS

The variation of the heat-transfer coefficient along the nozzle with the 18-in cooled-approach length is shown in Fig. 8 for stagnation temperatures of about 1030°, 1500°, and 2000°R and a range of stagnation pressures from 30 to 254 psia. At the highest stagnation temperature, it was not possible to obtain data above a stagnation pressure of 125 psia because of temperature limitations on the wall-thermocouple insulating material. The curves in Fig. 8 were faired through the data. It is evident that during a given test, circumferential variations in heat transfer did exist, as indicated by the symbols which are tagged in the same manner. These indicate thermocouple plugs spaced within 55° of each other. A certain amount of consistency can be deduced by comparing data obtained from the same thermocouple plugs for different tests. The majority of the tests were duplicated and found reproducible to within about ± 2 per cent. It was not possible to explain these variations by non-uniformities in the flow based on measurements in the gas stream at the nozzle inlet. However, it is possible that non-uniformities could have existed in the boundary layer.

The heat-transfer coefficients in Fig. 8 increase, as expected, with increasing stagnation

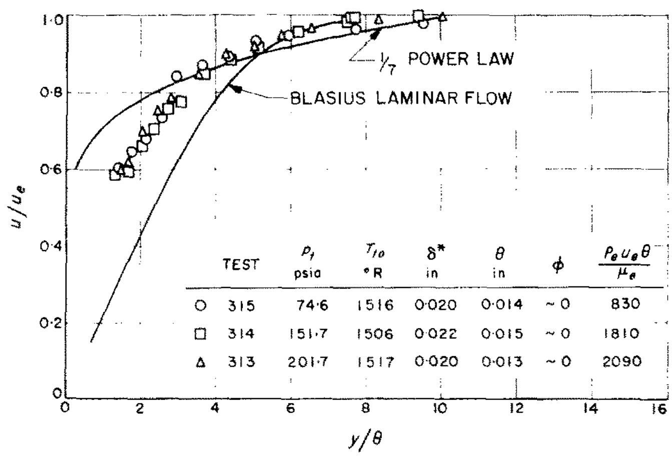

FIG. 7. Velocity profiles 1·25 in upstream of the nozzle inlet with no cooled-approach length.

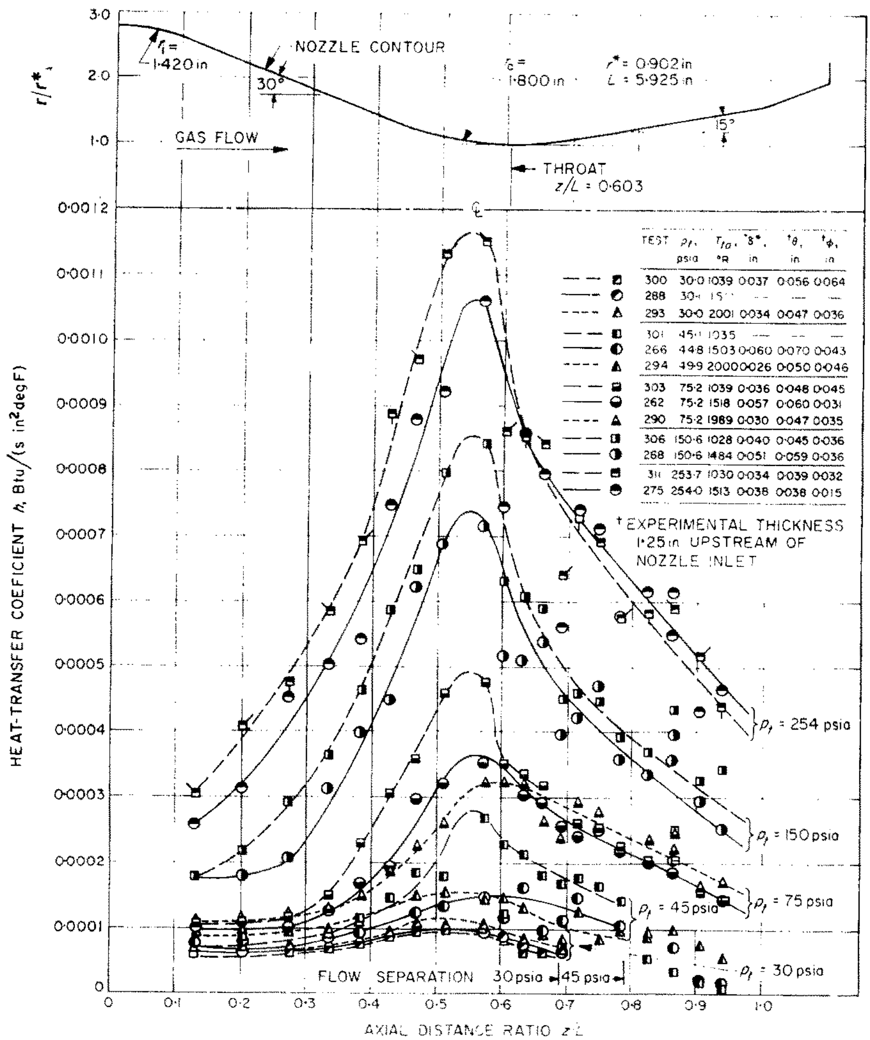

FIG. 8. Heat-transfer coefficient vs. axial-distance ratio with the 18-in cooled-approach length.

pressures as a result of larger mass fluxes; however, their variation with stagnation temperature at the different stagnation pressures is less clear, with the trends dependent on stagnation pressure. The maximum value of the heat-transfer coefficients occurs just upstream of the throat in the vicinity where the mass flux $\rho_e u_e$, as indicated in Fig. 5, is a maximum. A substantial decrease in heat transfer downstream of the point of flow separation which occurred at the low stagnation pressures is indicated by the tests at a stagnation pressure of 45 psia. At the lowest stagnation pressure, the data are not shown in this region, since there were large fluctuations in the wall-thermocouple readings.

To represent the heat-transfer results shown in Fig. 8 in terms of correlation parameters commonly used involves both the selection of a characteristic length and the temperature at which properties are evaluated. In Fig. 9 there are shown, in addition to the data of Fig. 8, data from many more tests at intermediate stagnation pressures presented in terms of the group, $St\, Pr^{0.6}$, and the Reynolds number based on the

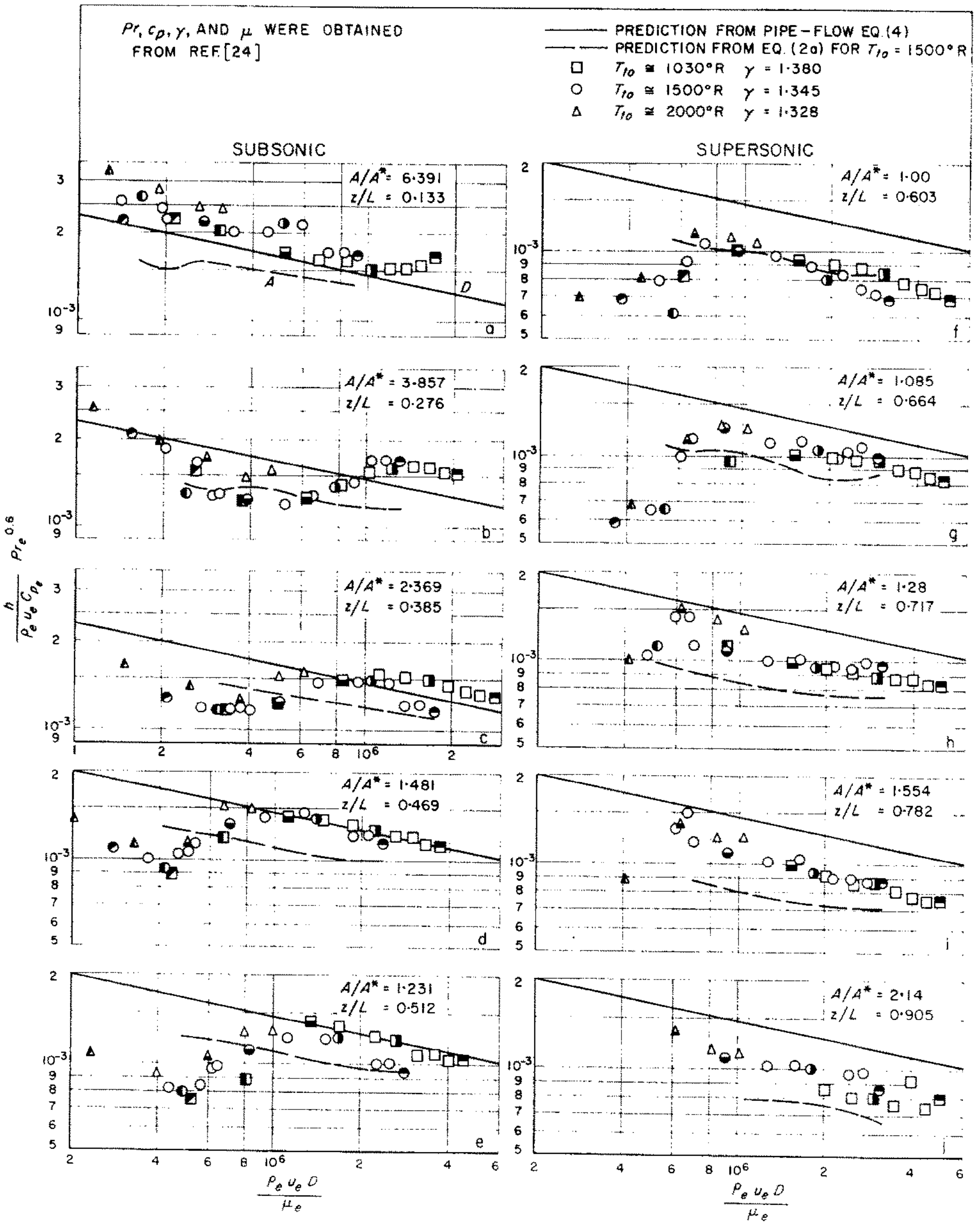

FIG. 9. Heat-transfer results at various subsonic and supersonic area ratios with the 18-in cooled-approach length.

local nozzle diameter. Fluid properties were evaluated at the static temperature at the edge of the boundary layer, and the mass flux $\rho_e u_e$ was used to compute both the Stanton and and Reynolds numbers. Each of the plots in Fig. 9 indicates the heat-transfer data obtained at a single area ratio or axial station. Hence, in each of the plots, increasing Reynolds numbers $\rho_e u_e D/\mu_e$ at the different stagnation temperatures correspond directly to increasing stagnation pressures, since the nozzle diameter is constant.

Proceeding through the subsonic part of the nozzle (decreasing area ratios), there is a substantial reduction in heat transfer at the lower stagnation pressures below that typical of a turbulent boundary layer, where the dependence of the heat-transfer coefficient on the mass flux is $h \propto (\rho_e u_e)^{4/5}$. This reduction persists through the throat and into the supersonic region before it diminishes near the nozzle exit. At the highter stagnation pressures, above 75 psia, the heat transfer is typical of a turbulent boundary layer.

Other investigators have observed unexpected trends accompanying the acceleration of turbulent boundary layers. The trends shown in Fig. 9 are similar to the results of reference 1 which were obtained from rocket-engine tests over a similar range of stagnation pressures. The large positive slope of the experimental curves at area ratios near 1 was noted as well as the eventual decrease in slope with increasing stagnation pressure. This implies that for the rocket-engine tests, injection and combustion effects which did influence the magnitudes of the heat fluxes did not substantially alter the heat-transfer trends from those indicated in Fig. 9. In reference 10, a turbulent boundary layer at the entrance of a supersonic nozzle was found to undergo transition to a nearly laminar one at the nozzle exit. The stagnation pressure was 4·3 psia. When the stagnation pressure was increased to 14·2 psia, a turbulent boundary layer was found at the nozzle exit. No boundary layer measurements were made within the nozzle. In reference 11, it was observed that heat-transfer trends of the type seen here at the low stagnation pressures existed under lower pressure-gradient conditions. There was departure from fully turbulent flow through the acceleration region as indicated by the linearity of the measured velocity profiles in the wall vicinity.

From these observations, it seems logical to speculate that at the lower stagnation pressures, the boundary layer may have undergone transition from the turbulent profile at the nozzle inlet to a partially laminar profile under the influence of the large, favorable pressure gradient. The consequent decrease in eddy transport would reduce both the wall friction and heat transfer. In the last Section, a parameter relating a predicted reduction in net production of turbulent kinetic energy to the low stagnation pressures is discussed.

The effect of varying nozzle-inlet boundary-layer thicknesses on the heat transfer is shown in Fig. 10, in particular for a stagnation temperature of 1500°R and stagnation pressures of 75 and 202 psia. With no cooled-approach length, for which the ratio of estimated boundary-layer thickness to nozzle-inlet radius is about 0·05, the heat-transfer coefficient is above the thicker layer results. This trend persists through the nozzle and extends into the supersonic region. Just upstream of the throat, where the heat-transfer coefficient is a maximum, the thinnest layer results exceed the thickest layer results obtained with the 18-in cooled-approach length by about 10 per cent. Apparently, with no cooled-approach length, transition from the boundary-layer profile shown in Fig. 7 to a turbulent one occurred upstream of the first heat-transfer measuring station.

COMPARISON OF HEAT-TRANSFER RESULTS WITH PREDICTIONS

Methods of predicting nozzle heat transfer consist either of boundary-layer analyses or, because of their simplicity, those related to pipe flow. In the boundary-layer analyses (e.g. [12, 13]), the integral forms of the momentum and energy equations are solved based on a number of assumptions, the most important of which is an assumed form of Reynolds analogy between heat transfer and wall friction. A limited amount of data [11, 14, 15] for heat transfer to an accelerated, essentially incompressible, turbulent boundary layer where property variations were small has indicated that heat-transfer coefficients determined from the wall friction through one of the analogies known to apply for constant free-stream velocity were far in excess of actual values. However, since boundary-layer measurements were not made in the nozzle, an experimental check was not possible.

Another, more recent, boundary-layer prediction method in which various heat-transfer assumptions can be compared to experimental results is a modification of the turbulent

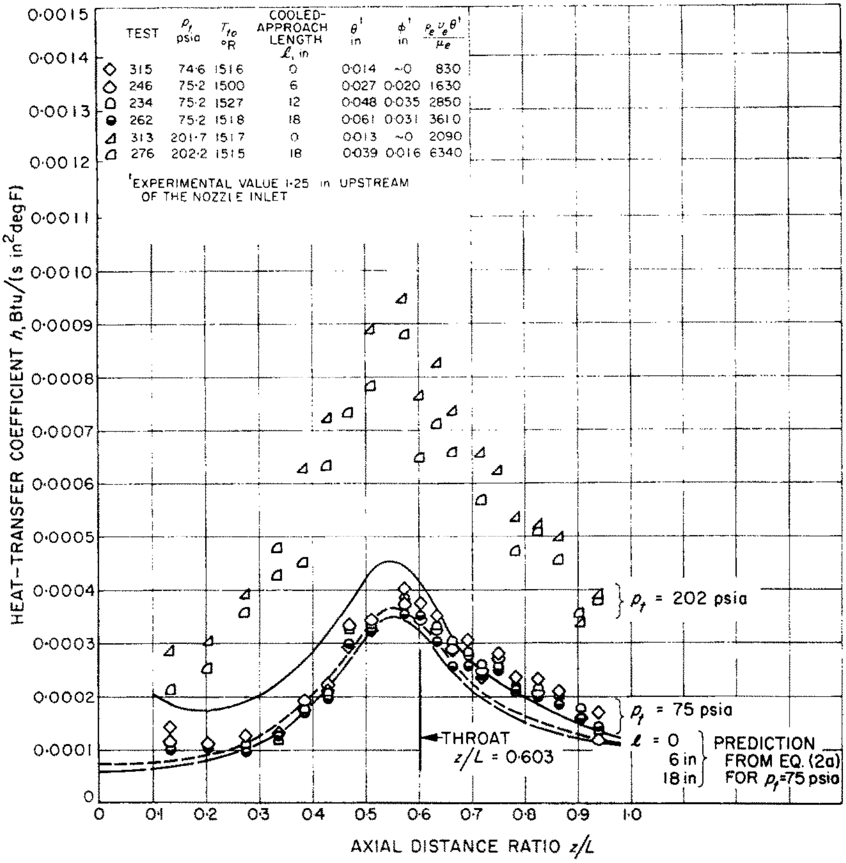

FIG. 10. Heat-transfer coefficients for various boundary-layer thicknesses at the nozzle inlet vs. axial-distance ratio.

boundary-layer analysis of reference 12. In the modified turbulent boundary-layer analysis, as in reference 12, the integral forms of the momentum and energy equations are solved simultaneously for θ and ϕ. The assumptions involve the specification of the heat-transfer and wall-friction coefficients, and the similarity of the boundary-layer velocity and stagnation-temperature profiles on a $\frac{1}{7}$-power-law basis with respect to their individual thicknesses, which can be different from one another. The prediction yields both the flow and thermal characteristics when the nozzle configuration, wall temperature, and free-stream properties are specified. To initiate the prediction, a knowledge of θ and the ratio of thicknesses δ_t/δ is required at one location near the nozzle inlet. A complete report on the computation procedure of the modified boundary-layer analysis, which is programmed for numerical solution on an IBM 7090 computer, is presented in reference 16.

The heat-transfer specification from the modified turbulent boundary-layer analysis [16] is

$$\frac{h}{\rho_e u_e c_p} = K^* \frac{c_f^*}{2} \left(\frac{\phi}{\theta}\right)^n \tag{2}$$

where

$$K^* = \left\{ \sqrt{\left(\frac{c_f^*}{2}\right)} \left[5\,Pr + 5 \ln (5\,Pr + 1) - 14 + \sqrt{\left(\frac{2}{c_f^*}\right)} \right] \right\}^{-1}.$$

The factor K^* is similar to the Prandtl-number correction factor in the von Kármán analogy. The coefficient c_f^* is analogous to the wall friction coefficient c_f but with the momentum thickness dependence replaced by the energy thickness. The ratio $(\phi/\theta)^n$ is a factor included in the analysis. For the present test results at stagnation pressures above 75 psia n was found to be near zero. The wall friction coefficient is predicted either from the Blasius flat-plate relation with properties ρ and μ evaluated at the film temperature, as was done in the earlier analysis [12], or by taking the adiabatic wall friction coefficient (predicted from Cole's relation [17] between the friction coefficient for a compressible and incompressible flow) with properties evaluated as in reference 16. This latter method is suggested by a limited amount of data [18] for low speed flow which indicate both the Stanton number and wall friction coefficient with properties evaluated at the free-stream temperature to be insensitive to severe wall cooling. Of note is that for a severely cooled wall, the friction coefficient predicted by the latter method is substantially below that predicted by evaluating properties at the film temperature.

To predict the heat-transfer coefficient from equation (2) requires the selection of n and the temperature at which properties are to be evaluated. With $n \simeq 0{\cdot}1$, the prediction is approximately the same as that of reference 12. For comparison purposes, two limiting values of n are considered. These correspond to assuming a Stanton-number dependence only on the thermal characteristic ϕ; i.e. $n = 0$, for which equation (2) becomes

$$\frac{h}{\rho_e u_e c_p} = K^* \frac{c_f^*}{2} \tag{2a}$$

or to taking $n = 0{\cdot}25$, for which equation (2) becomes approximately the von Kármán analogy

$$\frac{h}{\rho_e u_e c_p} = K \frac{c_f}{2} \tag{3}$$

where

$$K = \left\{ \sqrt{\left(\frac{c_f}{2}\right)} \left[5\,Pr + 5 \ln (5\,Pr + 1) - 14 + \sqrt{\left(\frac{2}{c_f}\right)} \right] \right\}^{-1}$$

Other analyses which assume a Stanton-number dependence on ϕ have been made in references 14 and 19 and compared to experimental heat-transfer results for accelerated turbulent boundary-layer flows. In reference 14, the predictions exceeded the data by about 30 per cent in part of the acceleration region, while in reference 19, the correspondence with the data was good.

The heat-transfer predictions shown in Fig. 11 as curve A are from equation (2a) for a stagnation temperature of 1500°R and a range of stagnation pressures from 45 to 254 psia, with the 18-in cooled-approach length. These predictions were made with properties evaluated as in reference 16 and conditions at the edge of the boundary layer determined from the wall static-pressure measurements. Shown as curve C in Fig. 11 is the prediction from equation (3), in which the friction coefficient $c_f/2$ was determined from the modified turbulent boundary-layer analysis. The reduction in the predicted heat-transfer coefficients provided by equation (2a) below the von Kármán analogy is due to the thicker predicted thermal than velocity boundary-layer thicknesses through the nozzle. At the highest stagnation pressure, the predicted ratios of ϕ/θ as indicated in Fig. 12 are as large as 6 in the throat region. At the 75-psia stagnation pressure, the correspondence of the prediction from the modified turbulent boundary-layer analysis equation (2a) with the data is good except near the nozzle exit. At the highest stagnation pressure of 254 psia, where the circumferential variation of the data is considerable, the correspondence with the averaged heat-transfer data is fair. The reproducibility of the data in Fig. 11 for 254 psia is indicated by the two sets of data shown by the open and shaded symbols. At the lowest stagnation pressure, $p_t = 44{\cdot}8$ psia, the prediction exceeds the data by as much as 50 per cent in the throat region. For the range of stagnation pressures, the predicted maximum value of the heat-transfer coefficient is just upstream of the throat, in agreement with the data.

The effect of temperature choice for property evaluation may be observed in Fig. 11 by comparing curves A and B. Curve B represents equation (2a) with properties evaluated at the

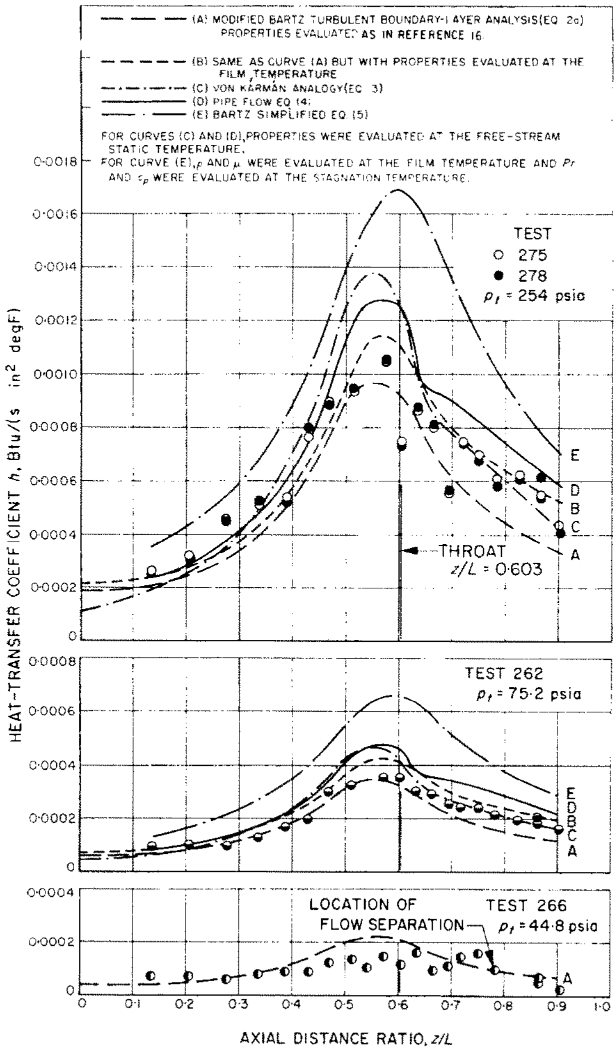

FIG. 11. Comparison of experimental heat-transfer coefficients with predictions at $T_{t_0} = 1500°R$ with the 18-in cooled-approach length.

film temperature T_f. In the throat region, it lies above the data, but is in better agreement near the nozzle exit than curve A.

For comparison purposes, the predictions from the following form of the pipe-flow equation for fully developed flow in which both the thermal and velocity boundary layers extend to the centerline and in which there is no significant pressure gradient are shown as curve D in Fig. 11.

$$St\, Pr^{0·6} = 0·023\, Re_D^{-0·2} \tag{4}$$

Also shown as curve E in Fig. 11 is the equation of reference 20.

$$h = \left[\frac{0·026}{(D^*)^{0·2}}\left(\frac{\mu^{0·2}c_p}{Pr^{0·6}}\right)_0\left(\frac{p_0 g_c}{c^*}\right)^{0·8}\left(\frac{D^*}{r_c}\right)^{0·1}\right]\left(\frac{A^*}{A}\right)^{0·9}\sigma. \tag{5}$$

In the pipe-flow equation, all properties were evaluated at the free-stream static temperature, while in equation (5), the Prandtl number and

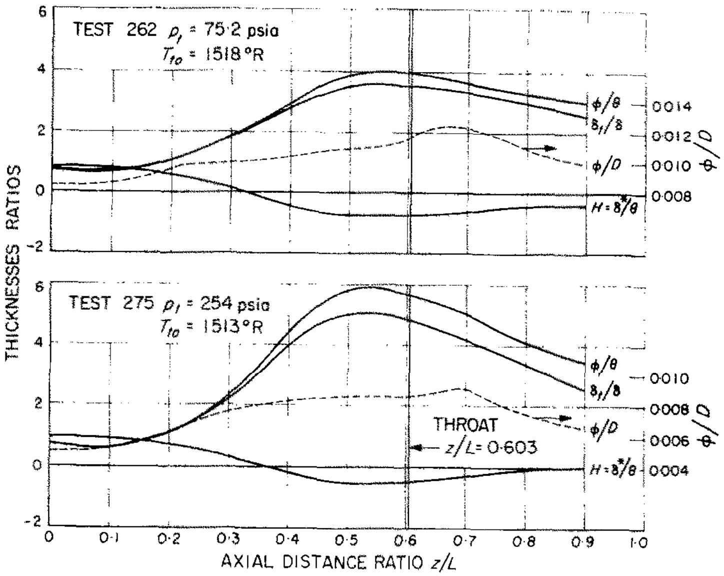

FIG. 12. Predicted thickness ratios along the nozzle with the 18-in cooled-approach length.

specific heat were assumed constant at their stagnation temperature values and ρ and μ were evaluated at the film temperature. In equation (5), one-dimensional flow quantities were used, since two-dimensional effects are not taken into account in the derivation. If they were, the prediction would be nearer that of the pipe-flow equation. Two-dimensional values of local mass flux are 15 per cent below the one-dimensional values just downstream of the nozzle throat, as seen in Fig. 5. The prediction from equation (5) exceeds the data by as much as 80 per cent in the throat region. The pipe-flow equation [equation (4)] prediction, though in better agreement with the data, is still about 25 per cent high at the throat.

From these observations, it appears that fair agreement with the data is provided at the higher stagnation pressures by the modified boundary-layer analysis taken in the form of equation (2a), with properties evaluated as in reference 16. These predictions are also shown, along with others at the intermediate pressures of $p_t = 60$ and 150 psia for $T_{t0} = 1500°$R as curve A in Fig. 9. The predicted Stanton-number dependence on the mass flux is approximately that of the pipe-flow equation, which is shown as curve D. However, an approximation cannot be made of the prediction for all the axial locations by an equation like the pipe-flow equation but with a lower coefficient. This is due to the variation of the predicted value of ϕ relative to D. For a given run, ϕ decreases through the subsonic region, attaining a minimum near the throat, and then increases in the supersonic region, qualitatively similar but not in direct correspondence with the nozzle diameter. A few of these predicted ratios are shown in Fig. 12.

In Figs. 9(c) through 9(i), the reduction in heat transfer at Reynolds numbers Re_D less than about 8×10^5 is not predictable from an analysis for a turbulent boundary layer, as indicated by the prediction from equation (2a) shown in Fig. 9 as curve A.

Predictions from equation (2a) were also made, though not shown, at stagnation temperatures of 1030° and 2000°R, with the 18-in cooled-approach length. The magnitude of the decrease in the heat-transfer coefficient with increasing stagnation temperature at the higher stagnation pressures shown in Fig. 8 was not predictable. From equation (2a), the dependence of the heat-transfer coefficient on stagnation temperature at a given stagnation pressure is nearly $h \propto T_{t0}^{-0\cdot 28}$ $\phi^{-0\cdot 2}$. However, the energy thickness at the nozzle inlet decreased with increasing stagnation temperature, such that the difference in predicted heat-transfer coefficients was substantially less than exhibited by the data.

The trend of higher heat-transfer coefficients through the nozzle with thinner boundary layers at the nozzle inlet is shown in Fig. 10 to be predictable from equation (2a). However, the magnitude of the predicted increase should probably be estimated from the 6- and 18-in cooled-approach length predictions. For the zero cooled-approach length prediction, wall cooling was assumed to begin at the nozzle inlet. To require that the Stanton numbers remain finite there, the energy thickness was taken at a small value equal to 0·001 in.

SOME ADDITIONAL OBSERVATIONS OF THE FLOW AND THERMAL CHARACTERISTICS

In this Section, some features of the flow are shown which depend on the predicted flow and thermal characteristics obtained from the modified turbulent boundary-layer analysis [16], with properties evaluated as in reference 16. In Fig. 12, the predicted ratios of ϕ/θ and δ_t/δ indicate the thicker predicted thermal than velocity boundary layers, especially in the throat region. Because of the cooled wall, the displacement thickness δ^* becomes negative upstream of the throat, as does $H = \delta^*/\theta$.

In Fig. 13, the predicted momentum thickness Reynolds numbers are a minimum a considerable distance upstream of the throat. At the lowest stagnation pressure, where the heat transfer is below that typical of a turbulent boundary layer, the minimum Reynolds number is 1500. Although this predicted value is probably different from the actual value, it is still considerably above the measured value of 600 found in reference 11 below which there was departure from fully turbulent flow. For the case of constant free-stream velocity, Preston [21] proposed a value of 320, above which the flow could be considered fully turbulent; for accelerated flows, he estimated that the limit might be lower.

To indicate the magnitude of the forces acting on the boundary layer through the nozzle, the ratio of the pressure forces which tend to accelerate the boundary-layer flow to the re-

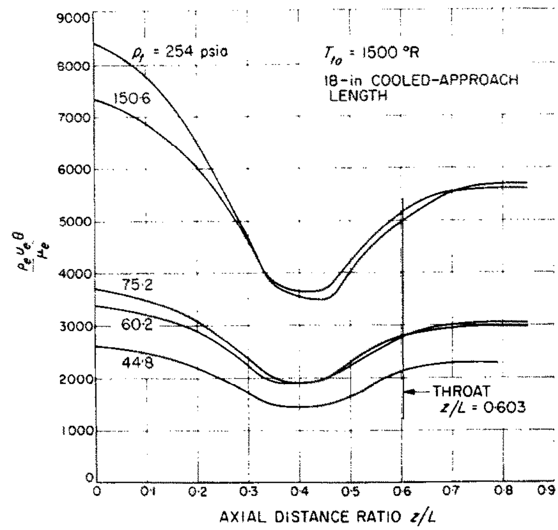

FIG. 13. Predicted momentum thickness Reynolds numbers along the nozzle.

tardation wall shear forces is shown in Fig. 14 as $-\{[\delta(\mathrm{d}p/\mathrm{d}x)]/\tau_w\}$. The ratio is largest in the convergent section before decreasing through the throat and divergent section. For comparison the value of the ratio for fully developed flow in a circular pipe is shown to demonstrate the large flow accelerations in a nozzle.

To gain some knowledge of the mechanism which at the low stagnation pressures reduces the heat transfer below that typical of a fully turbulent boundary layer, reference is made to the boundary-layer turbulence-energy equation (e.g. see [22]). For simplicity, an incompressible plane flow is assumed for which the convection of turbulent kinetic energy by the mean flow is

$$u_j \frac{\partial \overline{q^2/2}}{\partial x_j} = \underbrace{-\overline{u_i' u_j'} \frac{\partial u_i}{\partial x_j}}_{\text{(a)}} \underbrace{- \frac{\partial}{\partial x_j}}_{\text{(b)}} \underbrace{\overline{u_j' \left(\frac{p'}{\rho} + \frac{q^2}{2}\right)}}_{\text{(c)}} + \underbrace{\overline{\nu u_i' \frac{\partial^2 u_i'}{\partial x_j^2}}}_{\text{(d)}}. \qquad (6)$$

The terms represent the following:

(a) production of turbulent kinetic energy by the working of the mean velocity gradients against the Reynolds stresses

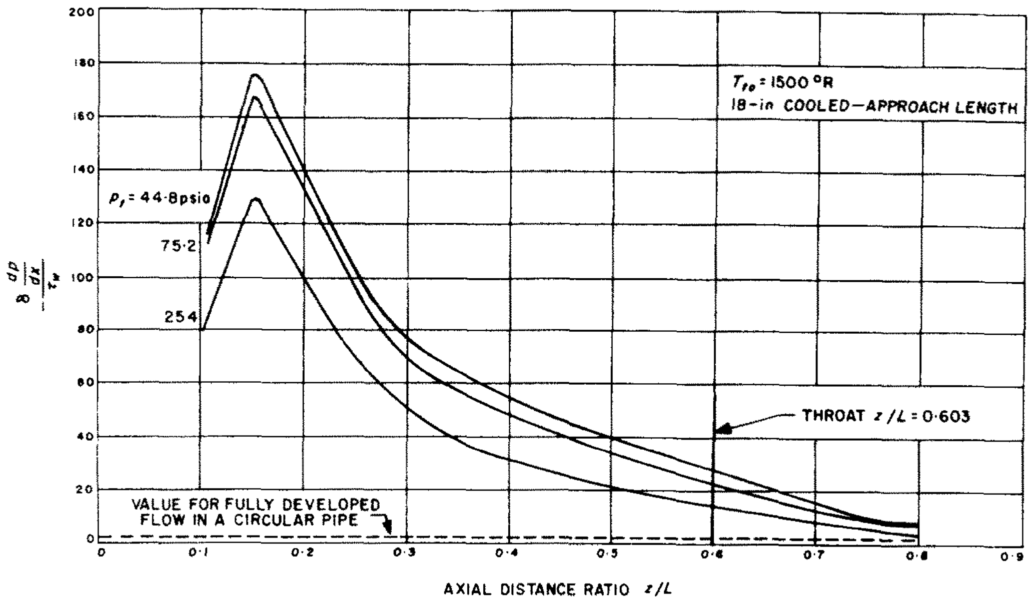

FIG. 14. Predicted ratio of pressure to wall shear forces acting on the boundary layer along the nozzle.

(b) work done by the turbulence against the fluctuation pressure gradients
(c) convection of turbulent kinetic energy by the turbulence itself
(d) transfer of energy by the working of the turbulent viscous stresses

For a two-dimensional flow with a pressure gradient the significant terms from term (a) that lead to a production or decay of convected turbulent kinetic energy are

$$-\overline{u_i'u_j'}\frac{\partial u_i}{\partial x_j} = -\overline{u'v'}\frac{\partial u}{\partial y} - (\overline{u'^2} - \overline{v'^2})\frac{\partial u}{\partial x}. \tag{7}$$

The remaining terms (b), (c) and (d) in equation (6) are dependent on the turbulence produced. The first term in equation (7) is always positive and leads to a production of turbulent kinetic energy. However, with flow acceleration $\partial u/\partial x > 0$, the second term leads to a decay of turbulent kinetic energy provided that $\overline{u'^2} > \overline{v'^2}$. Thus, a measure of the importance of flow acceleration in reducing the net production of turbulent kinetic energy is given by a ratio of the two terms in equation (7):

$$\chi = \frac{(\overline{u'^2} - \overline{v'^2})(\partial u/\partial x)}{-\overline{u'v'}(\partial u/\partial y)}. \tag{8}$$

To establish the variation of χ in the flow direction requires a knowledge of the turbulent quantities across the boundary layer. In the absence of turbulence measurements in accelerated flows, this estimate is restricted to the flat-plate measurements of Klebanoff [23] at a momentum thickness Reynolds number of about 8×10^3. The production term $\overline{-u'v'}\ \partial u/\partial y$ is largest in the wall vicinity where $[y\sqrt{(\tau_w/\rho_e)}]/\nu_e \simeq 30$. Using the "law of the wall",

$$\frac{u}{\sqrt{(\tau_w/\rho_e)}} = 5{\cdot}5 + 2{\cdot}5 \ln \frac{y\sqrt{(\tau_w/\rho_e)}}{\nu_e}$$

the velocity gradient is

$$\frac{\partial u}{\partial y} = \frac{2{\cdot}5}{30}\frac{\tau_w}{\rho_e \nu_e}.$$

An average value of $(\overline{u'^2} - \overline{v'^2})/\overline{-u'v'} \simeq 1{\cdot}8$ is taken from Klebanoff's data since this ratio did not vary appreciably across most of the boundary layer. Approximating the velocity gradient $\partial u/\partial x$ by its free-stream value du_e/dx

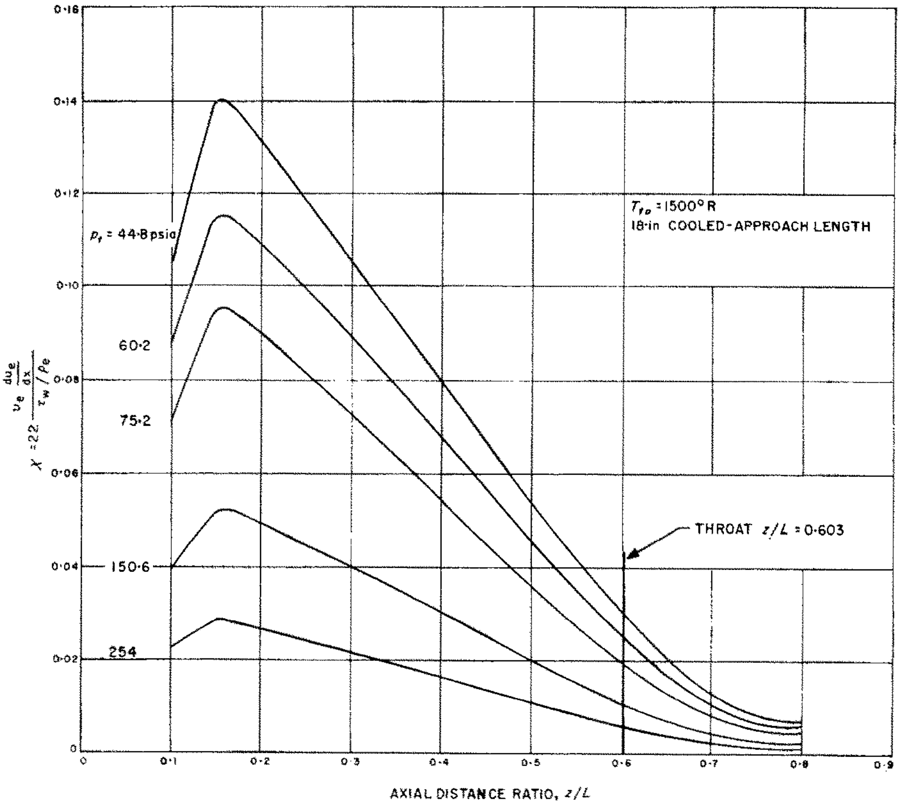

FIG. 15. Predicted effect of flow acceleration in reducing the net production of turbulent kinetic energy at different stagnation pressures.

and combining the other approximations gives

$$\chi \cong \frac{22\nu_e\,(\mathrm{d}u_e/\mathrm{d}x)}{(\tau_w/\rho_e)}.$$

Although the constant, 22, is somewhat arbitrary, the essential feature is the dependence of χ on the group,

$$\frac{\nu_e\,(\mathrm{d}u_e/\mathrm{d}x)}{(\tau_w/\rho_e)}.$$

The variation of χ along the nozzle is shown in Fig. 15 at $T_t = 1500°$R for the range of stagnation pressures from 45 to 254 psia. With decreasing stagnation pressure, the increasing values of χ indicate the predicted reduced net production of turbulent kinetic energy. At the lowest stagnation pressure, χ attains a maximum value of 0·14. Actually, for the low stagnation pressures, the values of χ should exceed those shown, since the low heat transfer implies that the wall shear is below the predicted value. The variation of χ along the nozzle displays the same trend of being largest in the convergent section before diminishing through the throat and divergent section as the departure of the heat-transfer data at the low stagnation pressures from that typical of a turbulent boundary layer observed in Fig. 9. The values of χ indicate when the turbulent shear stress, $\overline{u'v'}$, which is related to the turbulent kinetic energy, is expected to be lower than that typical of a fully turbulent boundary layer. The transport of heat would also be reduced, since it depends on the level of turbulent transport.

CONCLUSIONS

Experimental convective heat-transfer results have been presented for a turbulent boundary-layer flow through a cooled convergent-divergent nozzle. The scope of the investigation covered a wide range of stagnation pressures and temperatures as well as nozzle-inlet boundary-layer thicknesses. The experimental results indicated the following:

1. Heat-transfer coefficients increased with increasing stagnation pressure as a result of the larger mass fluxes, but only at stagnation pressures above about 75 psia were values typical of a turbulent boundary layer.
2. At low stagnation pressures, the heat-transfer coefficients were below that typical of a turbulent boundary layer even though the boundary layers at the nozzle inlet were turbulent.
3. The effect of stagnation temperature on heat transfer was less clear, with the trends dependent on stagnation pressure.
4. Heat-transfer coefficients were about 10 per cent higher throughout the nozzle with the thinnest boundary layer at the nozzle inlet ($\delta/R \simeq 0{\cdot}05$) than in the nozzle with the thickest inlet boundary layer ($\delta/R \simeq 0{\cdot}25$).
5. The heat-transfer coefficient is a maximum upstream of the throat, where the mass flux, deduced from wall static pressure measurements, is largest. Deviations of the mass flux from that predicted for one-dimensional flow amounted to as much as 15 per cent just downstream of the throat.
6. A substantial decrease in heat transfer existed downstream of the point of flow separation. Flow separation in the divergent portion of the nozzle occurred at the low stagnation pressures.

Various heat-transfer predictions were compared to the data. Fair agreement at the higher stagnation pressures is provided by a modification of the turbulent boundary-layer analysis of reference 12, in which the Stanton number is taken dependent on a Reynolds number based on a thickness characteristic of the thermal boundary layer. For the low stagnation pressures, where the turbulent boundary layer is thought to have undergone partial transition toward a laminar one, a parameter is found which is a measure of the importance of flow acceleration in reducing the transport of heat below that typical of a fully turbulent boundary layer.

More work is needed to gain some experimental knowledge of the flow and thermal boundary layers within a convergent–divergent nozzle and of the extent to which these are predictable by an analysis such as that of reference 16.

REFERENCES

1. A. B. WITTE and E. Y. HARPER, Experimental investigation of heat transfer rates in rocket thrust chambers, *AIAAJ.* **1**, 443–451 (1963). Also Technical Report No. 32–244, Jet Propulsion Laboratory, Pasadena, California, 19 March (1962.)
2. O. A. SAUNDERS and P. H. CALDER, Some experiments on the heat transfer from a gas flowing through a convergent–divergent nozzle, *Proceedings of the* 1951 *Heat Transfer and Fluid Mechanics Institute*, University Press, Stanford (1951).
3. W. C. RAGSDALE and J. M. SMITH, heat transfer in nozzles, *Chem. Engr. Sci.* **11**, 242 (1960).
4. J. R. BARON and F. H. DURGIN, An experimental investigation of heat transfer at the boundaries of supersonic nozzles. Naval Supersonic Laboratory, Massachusetts Institute of Technology, *WADC* Technical Report 54–541 (1954).
5. *Combined Bimonthly Summary No.* 63, *Dec.* 1, 1957 *to Feb.* 1, 1958, Jet Propulsion Laboratory, Pasadena, pp. 28–30, Feb. 15 (1958). *Combined Bimonthly Summary No.* 65, *April* 1, 1958 to *June* 1, 1958, Jet Propulsion Laboratory, Pasadena, p. 32, 15 June (1958).
6. J. J. KOLOZSI, An investigation of heat transfer through the turbulent boundary layer in an axially symmetric, convergent–divergent nozzle. Aerodynamic Lab., Ohio State University, *TM*-8, July 1958.
7. J. L. LIVESEY, The behavior of transverse cylindrical and forward-facing pressure probes in transverse total pressure gradients, *J. Aero. Sci.* **23**, 949–955 (1956).
8. R. A. SEBAN and D. DOUGHTY, Heat transfer to laminar and turbulent boundary layers with constant and variable free-stream velocity. University of California, Institute of Engineering Research, Series 41, No. 13, August 1954.
9. K. OSWATITSCH and W. ROTHSTEIN, Flow pattern in a converging–diverging nozzle, *NACA TM*-1215 (1949).
10. A. A. SERGIENKO and V. K. GRETSOV, Transition from a turbulent into a laminar boundary layer, *Sov. Phys. Dokl.* **4**, 275–276 (1959).
11. L. H. BACK, Heat transfer to turbulent boundary layers with a variable free-stream velocity. Ph.D. Thesis, University of California, Berkeley, California, June 1962.
12. D. R. BARTZ, An approximate solution of compressible turbulent boundary-layer development and convective heat transfer in convergent–divergent nozzles, *Trans. ASME*, **77**, 1235–1245 (1955).
13. E. RESHOTKO and M. TUCKER, Approximate calculation of the compressible turbulent boundary layer

with heat transfer and arbitrary pressure gradient. *NACA TN*-4154 (1957).
14. R. A. SEBAN and H. W. CHAN, Heat transfer to boundary layers with pressure gradients. University of California, Institute of Engineering Research, Series 41, No. 16 (1957).
15. T. F. MCCARTHY, Heat transfer to turbulent boundary layers with a pressure gradient. Master's Thesis, University of Minnesota (1960).
16. D. G. ELLIOTT, D. R. BARTZ and S. SILVER, Calculation of turbulent boundary-layer growth and heat transfer in axi-symmetric nozzles. Technical Report No. 32-387, Jet Propulsion Laboratory, Pasadena (1963).
17. D. E. COLES, The turbulent boundary layer in a compressible fluid. Report No. *P*-2417, The Rand Corporation, Santa Monica, California (1961).
18. H. WOLF, The experimental and analytical determination of the heat transfer characteristics of air and carbon dioxide in the thermal entrance region of a smooth tube with large temperature differences between the gas and the tube wall. Ph.D. Thesis, Purdue University, Lafayette, Indiana, March 1958. Also *ASME J. Heat Transfer*, **81**, 267–269 (1959).
19. S. S. KUTATELADZE and A. I. LEONTEV, Drag law in a turbulent flow of a compressible gas and the method of calculating friction and heat exchange. *Akad. Nauk, Belorussk, S.S.S.R.*, Minsk, 1–23, 23–27, Jan. 1961, U.S.S.R.; Translated and issued by Technical Information and Library Services, Ministry of Aviation, Dec. 1961.
20. D. R. BARTZ, A simple equation for rapid estimation of rocket nozzle convective heat-transfer coefficients. *Jet Propulsion*, **27**, 49–51 (1957).
21. J. H. PRESTON, The minimum Reynolds number for a turbulent boundary layer and the selection of a transition device, *J. Fluid Mech.*, **3**, 373–384 (1958).
22. J. O. HINZE, *Turbulence*, p. 62. McGraw-Hill, New York (1959).
23. P. S. KLEBANOFF, Characteristics of turbulence in a boundary layer with zero pressure gradient, *NACA TN*-3178, 1954.
24. J. H. KEENAN and J. KAYE, *Gas Tables*. John Wiley, New York (1956).

Résumé—On présent les résultats d'une investigation experimentale du transport convective de chaleur par des couches limites turbulents, accélérés par des larges gradients de pression dans une tuyère refraîchie convergente–divergente. Les investigations se sont étendues sur les pressions de stagnation entre 30 et 250 psia,† sur les températures de stagnation entre 1030° et 2000°R, et sur des épassieurs de la couche limite entre 5–25 pour cent du rayon de l'entrée. La tendance inattendue la plus importante dans les résultats est la reduction du coefficient du transport de chaleur à une valeur au dessous de celle caractéristique pour une couche limite turbulente, à des pressions au dessous d'environ 75 psia.† Comme attendu, les résultats englobent un maximum du coéfficient du transport de chaleur avant de la gorge oú la vitesse du courant de masse est la plus grande par unité de surface, et une décroissance substantielle du coéfficient du transport de chaleur après le point de séparation du courant. Ce point se trouve dans la section divergente de la tuyère pour les pressions de stagnation basses. Une réduction d'environs 10 pour cent dans le coefficient du transport de chaleur est due à une augmentation de l'épaisseur de la couche limite à l'entrée, entre les épaisseurs minimaux et maximaux.

Les prédictions du transport de chaleur, avec lesquelles les résultats sont comparés, soit incorporent une prédiction des particularités de la couche limite, soit elles sont rapportés au courant dans un tuyau. Aux pressions plus élevées, les valeurs prévues par une modification de la théorie de Bartz pour la couche limite turbulente sont assez proches avec les resultats. Comme explication possible du transport de chaleur bas aux pressions plus petites, on trouve un paramètre qui est une mesure de l'importance de l'accéleration du courant dans la reduction du transport turbulent au dessous duquel caractéristique pour une couche limite entièrement turbulente.

Zusammenfassung—Die Resultate einer experimentellen Untersuchung der Konvektionswärmeübertragung der turbulenten Grenzschicht, die beschleunigt wird unter dem Einfluss grosser Druckgradienten welche in einer gekühlten konvergent–divergenten Düse entstehen, werden beschrieben. Die Untersuchung umfasst den Gesamtdruckbereich 30 bis 250 psia† und den Stautemperaturbereich 1030° bis 2000°R. Die Grenzschichtdicke am Düseneingang lag zwischen 5 Prozent und 25 Prozent des Eingangradius. Das bedeitsamste, unerwartete Resultat der Untersuchung besteht in der Abnahme des Wärmeübertragungskoeffizienten unter demjenigen, der typisch ist für die turbulente Grenzschicht, bei Gesamtdrucken die unter etwa 75 psia† liegen. Wie erwartet, erreicht der Wärmeübertragungskoeffizient ein Maximum stromaufwärts vom Hals wo die Massenfliessdichte am grössten ist. Ebenso erleidet er eine bedeutende Abnahme stromabwärts vom Teilungspunkt des Stromes, welcher Punkt im divergenten Teil der Düse lag bei niedrigen Gesamtdrucken. Durch eine Zunahme der Eingangsgrenzschichtdicke, innerhalb des untersuchten Dickebereiches, nahm der Wärmeleitungskoeffizient um circa 10 Prozent ab.

Die theoretischen Voraussagen, mit denen die Messresultate verglichen wurden, sind entweder auf Strömungen in Röhren basiert oder geben Auskunft über die Eigenschaften der Grenzschicht. Bei

† 100 psia = 7,03 kg/cm² abs.

höheren Gesamtdrucken zeigen die Resultate ziemlich gute Übereinstimmung mit einer modifizierten Bartz'schen Theorie der turbulenten Grenzschicht. Um die niedrige Wärmeübertragung bei kleineren Gesamtdrucken zu erklären, wird ein Parameter definiert der ein Mass für die Strömungsbeschleunigung ist, die an der Reduktion des turbulenten Transportes unter demjenigen einer voll ausgebildeten turbulenten Grenzschicht beteiligt ist.

Аннотация—Представлены результаты экспериментального исследования конвективного переноса тепла в турбулентном пограничном слое при наличии больших градиентов давления в охлаждаемом сверхзвуковом сопле. Исследование проводилось в диапазоне абсолютного давления торможения от 30 до 250 фунт/кв. дюйм, температура торможения изменялась от 1030° до 2000°R. Толщина пограничного слоя во входной части составляла от 5 до 25% радиуса. Неожиданным результатом, представляющим большое значение, явилось уменьшение коэффициента теплообмена при абсолютном давлении торможения ниже 75 фунт/кв. дюйм по сравнению со значениями коэффициентов теплообмена, присущими турбулентному пограничному слою при безградиентном обтекании. Как и предполагалось, коэффициент переноса тепла имеет максимальное значение в горловине сопла, где наблюдается наибольший массовый расход потока на единицу площади, и значительно уменьшается вниз по потоку от точки отрыва, который происходит при низком давлении торможения в расходящейся части сопла. Уменьшение (до 10%) значения коэффициента теплообмена происходит в результате увеличения толщины пограничного слоя во входной части.

Теоретические расчеты по теплообмену, с которыми сравнивались экспериментальные данные, включают либо расчет характеристик пограничного слоя, либо относятся к течению внутри трубы. При больших давлениях торможения расчетные значения, полученные с помощью модификации анализа турбулентного пограничного слоя, проведенного Берцем, хорошо согласуются с экспериментальными данными. Найден параметр, который характеризует влияние ускорения потока на снижение турбулентного переноса ниже значений, присущих полностью турбулентному пограничному слою при градиентном течении.